Journal of Geoscience and Environment Protection, 2024, 12, 115-134
https://www.scirp.org/journal/gep
ISSN Online: 2327-4344
ISSN Print: 2327-4336

Correlation of Rainfall Anomalies in Rwanda from September to December (SOND) with Indian Ocean Dipole (IOD) and El Nino Southern Oscillation (ENSO) Events

Frank Rusanganwa[1,2*], Ling Zhang[1], Jonah Kazora[1,2], Joseph Ndakize Sebaziga[3], Samuel Ekwacu[1,4]

[1]College of Atmospheric Science, Nanjing University of Information Science and Technology, Nanjing, China
[2]Rwanda Meteorology Agency (Meteo-Rwanda), Kigali, Rwanda
[3]School of Science and Technology, University of Rwanda, Kigali, Rwanda
[4]Uganda National Meteorological Authority (UNMA), Kampala, Uganda
Email: *franklin02joe@ymail.com

How to cite this paper: Rusanganwa, F., Zhang, L., Kazora, J., Sebaziga, J. N., & Ekwacu, S. (2024). Correlation of Rainfall Anomalies in Rwanda from September to December (SOND) with Indian Ocean Dipole (IOD) and El Nino Southern Oscillation (ENSO) Events. *Journal of Geoscience and Environment Protection, 12,* 115-134.
https://doi.org/10.4236/gep.2024.126008

Received: April 27, 2024
Accepted: June 23, 2024
Published: June 26, 2024

Abstract

Understanding the relationship between rainfall anomalies and large-scale systems is critical for driving adaptation and mitigation strategies in socioeconomic sectors. This study therefore aims primarily to investigate the correlation between rainfall anomalies in Rwanda during the months of September to December (SOND) with the occurrences of Indian Ocean Dipole (IOD) and El Nino Southern Oscillation (ENSO) events. The study is useful for early warning and forecasting of negative effects associated with extreme rainfall anomalies across the country, using Climate Hazards Group InfraRed Precipitation with Station (CHIRPS), the National Centers for Environmental Prediction (NCEP) National Center for Atmospheric Research (NCAR) reanalysis sea surface temperature and ERA5 reanalysis datasets, during the period of 1983-2021. Both empirical orthogonal function (EOF), correlation analysis and composite analysis were used to delineate variability, relationship and the related atmospheric circulation between Rwanda seasonal rainfall September to December (SOND) with Indian Ocean Dipole (IOD) and El-Nino Southern Oscillation (ENSO). The results for Empirical Orthogonal Function (EOF) for the reconstructed rainfall data set showed three modes. EOF-1, EOF-2 and EOF-3 with their total variance of 63.6%, 16.5% and 4.8%, Indian ocean dipole (IOD) events resulted to a strong positive correlation of rainfall anomalies and Dipole model index (DMI) ($r = 0.42$, p value = 0.001, DF = 37) significant at 95% confidence level. The composite analysis for the reanalysis dataset was carried out to show the circulation patterns during four different events correlated with September to December seasonal rainfall in Rwanda using T-test at 95% confidence level. Wind anomaly revealed that there was a convergence of south westerly winds and easterly wind over the study area during positive Indian Ocean Diploe (PIOD) and PIOD with El Nino concurrence event years. The finding of this study will contribute to the enhancement of SOND seasonal rainfall forecasting and the reduction of vulnerability during IOD (ENSO) event years.

Keywords

Correlation, Rainfall Anomalies, Rwanda, Indian Ocean Dipole, El Nino Southern Oscillation

1. Introduction

Rainfall and its unpredictability are critical to agricultural activity in African countries including Rwanda, because the sector is rainfall-dependent. Agriculture is an important economic sector, dependent on rainfall regimes that are mainly unpredictable, highly variable, and seasonal in character (Akpoti et al., 2016; Ongoma et al., 2015; Wainwright et al., 2020). Rainfall variability in Africa has been seen to be seasonal, inter-annual, and decadal (Li et al., 2016; Nicholson, 2019). El Nino-Southern Oscillation (ENSO), a natural phenomenon connected with sea surface temperatures in the Tropical Pacific, is the primary cause of this fluctuation in rainfall in the sub-region and the tropics in general. The term Southern Oscillation (SO) is commonly used to describe a planetary scale phenomenon that involves a seesaw in surface pressure between Indonesia and the southeast Pacific (Ogallo, 1988; Yang et al., 2018). El Nino is the strongest inter-annual climate variation in the tropical Pacific air-sea coupled system, occurring at irregular intervals of two to seven years and lasting nine months to two years; it is well known for its association with natural disasters in far-flung parts of the world (Liang, 2014; Bayable et al., 2021). The term ENSO cycle describes how the air circulation and weather patterns change over a very large area together with the increase, peak, and decrease of sea surface temperature anomalies in the eastern and central Pacific (Mcgregor, 2018). Indian Ocean Dipole (IOD) on the other hand, is another air-sea coupled climate mode in the Indian Ocean, characterized by an aperiodic oscillation of sea surface temperature (SST). It has been linked to floods in East Africa, as well as droughts in Indonesia and parts of Australia. The Dipole Mode Index (DMI) is used to calculate Indian Ocean Dipole (IOD) (Moihamette et al., 2022). Indian Ocean Dipole is typically regarded as an independent mechanism of coupled ocean-atmosphere climate variability since it is largely driven by local ocean-atmosphere interactions rather than being a direct response to outside factors like El Nino Southern Oscillation (ENSO) (Saji et al., 1999). It has long been recognized that the tropical Indian and Pacific Oceans are interrelated on their Sea Surface Temperature anomalies

(Liang, 2014; Zhang et al., 2022; Marchant et al., 2007) indicated that the frequency of El Nino and IOD convergence has increased significantly since the 1980s. However, the frequency of La Nina and negative Indian Ocean Dipole (NIOD) convergence shows little variation. ENSO events can form in early summer, producing a lower-level anticyclone over the northwestern Indian Ocean, affecting the East African coast. However, if they begin in late summer or early fall, they create anomalous lower-level cyclones, limiting their ability to warm the western Indian Ocean (Fan et al., 2017). The Indian Ocean has a considerable impact on East Africa's precipitation regime during the "short rains" in September, October, November and December, with the amount of precipitation governed by the variability of the nearby ocean, namely the Indian Ocean dipole mode (Blau & Ha, 2020; Jiang et al., 2021; Liu et al., 2020).

Rwanda's natural resource systems, particularly lakes, marshes, and rivers, have been significantly impacted by rainfall changes. Rainfall is bimodal over much of East Africa (EA), with rainy seasons from March to May (MAM) and September to December (SOND), mitigated by coastal and topography effects (Conway et al., 2005). With increasing distance from the equator, the bimodal regime progressively transforms into a single season. Both the MAM and SOND rainfall regimes, as well as the transitional phase, indicate varied degrees of influence from the Atlantic, Indian, and Pacific Oceans. The SOND season in East Africa is heavily influenced by the intricate interaction of the Indian and Pacific oceans and has greater internal variability than the MAM. Periodic circulation dipole episodes in the Indian Ocean are connected with above-average and occasionally excessive rainfall from SOND (Webster et al., 1999). In comparison to the MAM, commonly termed "long rains" in EA, the SOND, commonly termed "short rains" in EA, have less rainfall but higher inter-annual variability and more spatial coherence of rainfall anomalies across a substantial portion of the region (Clark et al., 2003). We picked the SOND sub-season for analysis not only because it coincides with the peak period of Indian Ocean Dipole (IOD) activity, but also because it has a higher impact on communities due to changes in the regional hydrological cycle. Because of its increased variability, it is also less reliable. As a result, gaining a better knowledge of its decadal to multi-decadal variability may improve long-term forecasting of this season (Manatsa et al., 2012; Nyenzi, 1988). The objective of this study is to explore the correlation between rainfall anomalies in Rwanda during the months of September to December (SOND) and the occurrences of Indian Ocean Dipole (IOD) and El Niño Southern Oscillation (ENSO) events.

Study Area

Rwanda is located in central Africa, immediately south of the equator between latitudes 1˚4' and 2˚51'S and longitude 28˚63' and 30˚54'E. It has a surface area of 26,338 square kilometers and is bordered by Uganda to the north, Tanzania to the east, the Democratic Republic of the Congo to the west, and Burundi to the south. It is dominated topographically by the volcanic highlands in the north and west, and the lowlands in the Savannah region in the east and southeast (Figure 1). The highland region receives substantial rainfall, with a long-term mean of more than 1300 mm per year, but the savannah zone receives just ≤1000 mm per year. The country has two rainy seasons, the longer of which lasts from March to mid-May and the shorter of which lasts from mid-September to mid-December (Jonah et al., 2021). Subtropical anticyclones, tropical cyclones, Indian Ocean Dipole, monsoons, the El Nino Southern Oscillation (ENSO), significant water bodies, and terrain are all known to influence rainfall in Rwanda (Ngarukiyimana et al., 2017). These features expose Rwanda to unpredictable meteorological conditions, including frequent extreme rainfall occurrences.

2. Methodology and Data

2.1. Data

This study uses seasonal anomalies sourced from different dataset, UCSB-Chirps v2p0 (0.05˚ × 0.05˚) monthly global precipitation data, the IOD index (DMI) constructed by the SST anomalies (SSTA) gradient between the western (10˚S - 10˚N, 50˚E - 70˚E) and the eastern (10˚S - 0˚N, 90˚E - 110˚E) regions of Indian Ocean for the period from 1983-2021 was sourced from NOAA ERSSTv5 (2˚ × 2˚) resolution (Shi and Wang, 2021), the Nino-3.4 SST index is a sea surface

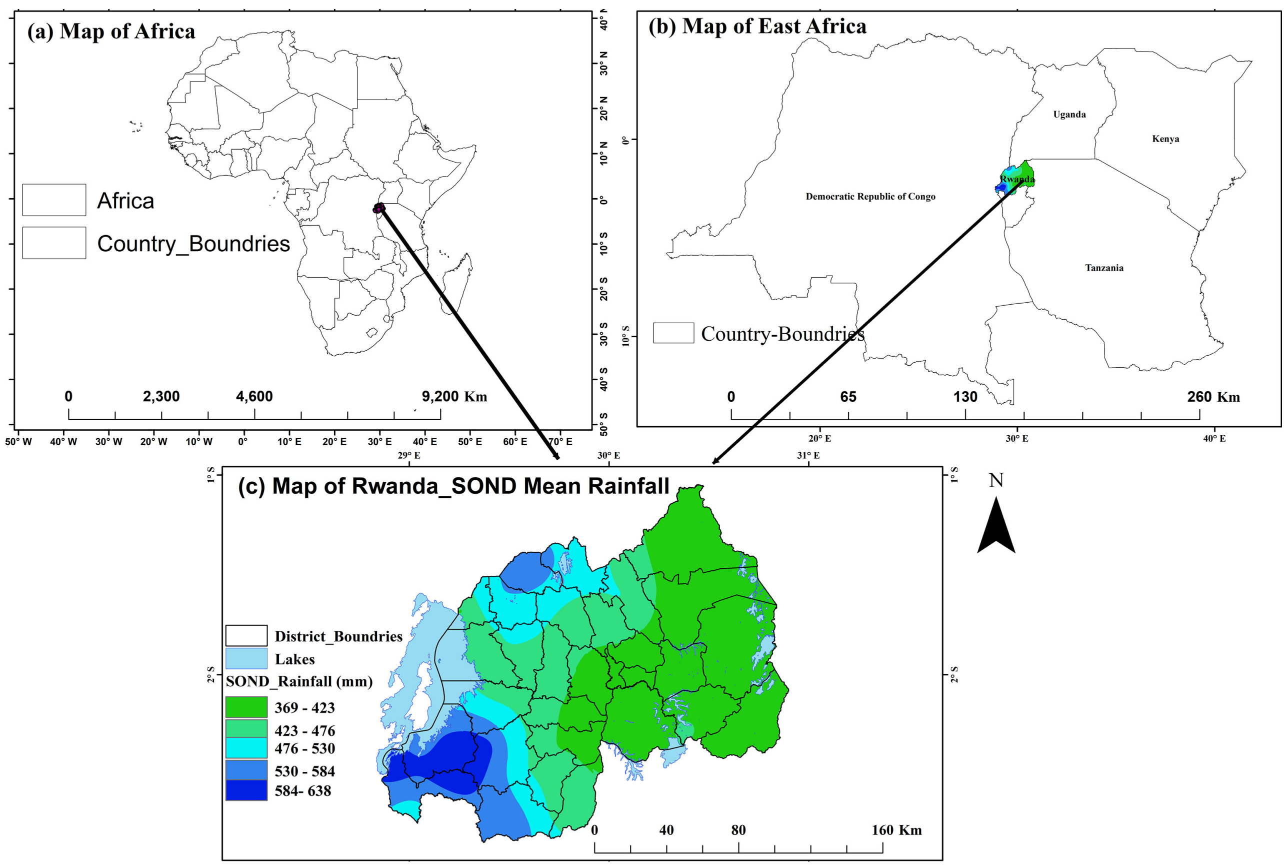

Figure 1. (a) Map of Africa showing where Rwanda is located, (b) East Africa map and (c) September to December seasonal mean rainfall (mm) over Rwanda.

temperature anomaly averaged over the region bounded by 5˚N to 5˚S and 170˚W to 120˚W in the eastern central equatorial Pacific (Stern & Cooper, 2011; Piao et al., 2020) Sourced:
(https://origin.cpc.ncep.noaa.gov/products/analysis_monitoring/ensostuff/ONI_v5.php) and atmospheric circulation data sourced from ERA5 (0.25˚ × 0.25˚) reanalysis dataset. All dataset used in this study will be analyzed for the period 1983-2021 using seasonal anomaly data.

Sea Surface Temperatures Index (SST's Index)

El Nino and La Nina years are defined according to the value of the Nino-3.4 index averaged over the season of interest. It is important to mention that El Nino can be explained as follows: The Nino-3.4 SST index is a sea surface temperature anomaly averaged over the region bounded by 5˚N to 5˚S and 170˚W to 120˚W in the eastern central equatorial Pacific (Stern & Cooper, 2011; Chen et al., 2018; Piao et al., 2020). It is one of several standard SST indices associated with El Nino/Southern Oscillation, which is an interaction between the atmosphere and ocean in the tropical pacific that results in variations between below-normal and above-normal conditions over the year in different parts of the World (Ntirenganya, 2016). The Nino 3.4 index will be considered when the index value is great or less than (−1) 1. Source:
(https://origin.cpc.ncep.noaa.gov/products/analysis_monitoring/ensostuff/ONI_v5.php).

The IOD index (DMI) constructed by the SST anomalies (SSTA) gradient between the western (10˚S - 10˚N, 50˚E - 70˚E) and the eastern (10˚S - 0˚, 90˚E - 110˚E) regions of Indian Ocean (Shi & Wang, 2021), Because an IOD event often develops in the summer, peaks in the autumn, and rapidly declines in the winter (Saji et al., 1999). In this study the years with a typical positive and Negative Indian Ocean Dipole, PIOD (NIOD) will be considered when the normalized DMI is great (less) 1 (−1).

2.2. Methodology

To assess the variability in the precipitation dataset, the empirical Orthogonal Function (EOF) was used to determine several purposes that designate most of the variance in the data and which can separate the leading modes from the remaining variability data (Gallaudet & Simpson, 1994).

In this study the Pearson linear correction coefficient was performed to analyses the relationship between the Rwanda September to December termed as "short rain" season (SOND) anomalies with Indian Ocean Dipole (IOD) and El-Nino Southern Oscillation (ENSO) events, during Positive Indian Ocean Dipole (PIOD) with El-Nino years, PIOD years, Negative Indian Ocean Dipole (NIOD), and NIOD with La-Nina years. Coefficient of correlation measures the intensity or degree of linear relationship between two variables. It was given by British Biometrician Karl Pearson (1867-1936) (Asuero et al., 2006).

To investigate how the Indian-Pacific Sea surface temperatures influence September to December seasonal rainfall in Rwanda. The wind anomalies are subjected to the composite analysis to assess the moisture transport during IOD and ENSO events. The classification of one or more classes of fields of a variable based on their suggestion with main conditions is included in composite analysis. The composite results are then used to generate hypotheses for patterns that may be related to the individual scenarios (Gunta et al., 2022). This explains why, if the mean value of the data is calculated in some ingenious way in relation to the event, the event signal continues and all other impacts tend to average out for a climate composite, this can be accomplished by combining the weather over a large area over many years using an index such as the IOD, ENSO index or the Precipitation Index to study the variation of weather phenomena such as precipitation, wind, or temperature. The first critical step is to choose a compositing basis (time basis), such as an hour of the day or a month of the year, and to define cyclic phenomena (categories). The mean and statistics for each category are then computed. Lastly, arithmetical significance is determined by using a two-tailed student's t-test then organizes and displays the results to which they are validated for their significance.

3. Results

3.1. Climatology of Rwanda

Figure 2 represents the country's rainfall pattern, with "long rains" occurring from March to May (MAM) and "short rains" occurring from September to December (SOND) (Jonah et al., 2021; Uwimbabazi et al., 2022). The yearly rainfall ranges from 700 mm to 1600 mm, with the southwest and northwest of Rwanda receiving the most. The eastern region of the nation experienced less annual precipitation. The central region of the country experiences moderate rainfall, averaging between 1000 to 1300 mm. The eastern region of the country experienced the least quantity of rainfall throughout both monthly, season and annual. In conclusion, the country's rainfall distribution has a southwest to northeast inclination. The temporal distribution of monthly rainfall (mm) from CHIRPS is depicted in **Figure 2(c)**; April and November show the largest amounts of rainfall. The driest months throughout the study period were June, July, and August. The months with the most rainfall in the nation are March, April, May, October, November, and December. This research and Previous research such as (Nicholson, 2019; Camberlin et al., 2009; Camberlin & Philippon, 2002) can be used to establish atmospheric circulations related to seasonal rainfall climatology over Rwanda and east Africa in general.

3.2. The Spatial the Temporal Distribution Characteristics of Rainfall in Rwanda during SOND

The empirical orthogonal function was estimated as a kind of eigenvector that is situated so the dominant EOF reports the spatially rational pattern that enlarges its alteration. Applying EOF helped to identify the first leading mode of alteration, reflecting mainly variations in strength and the latitudinal circulations

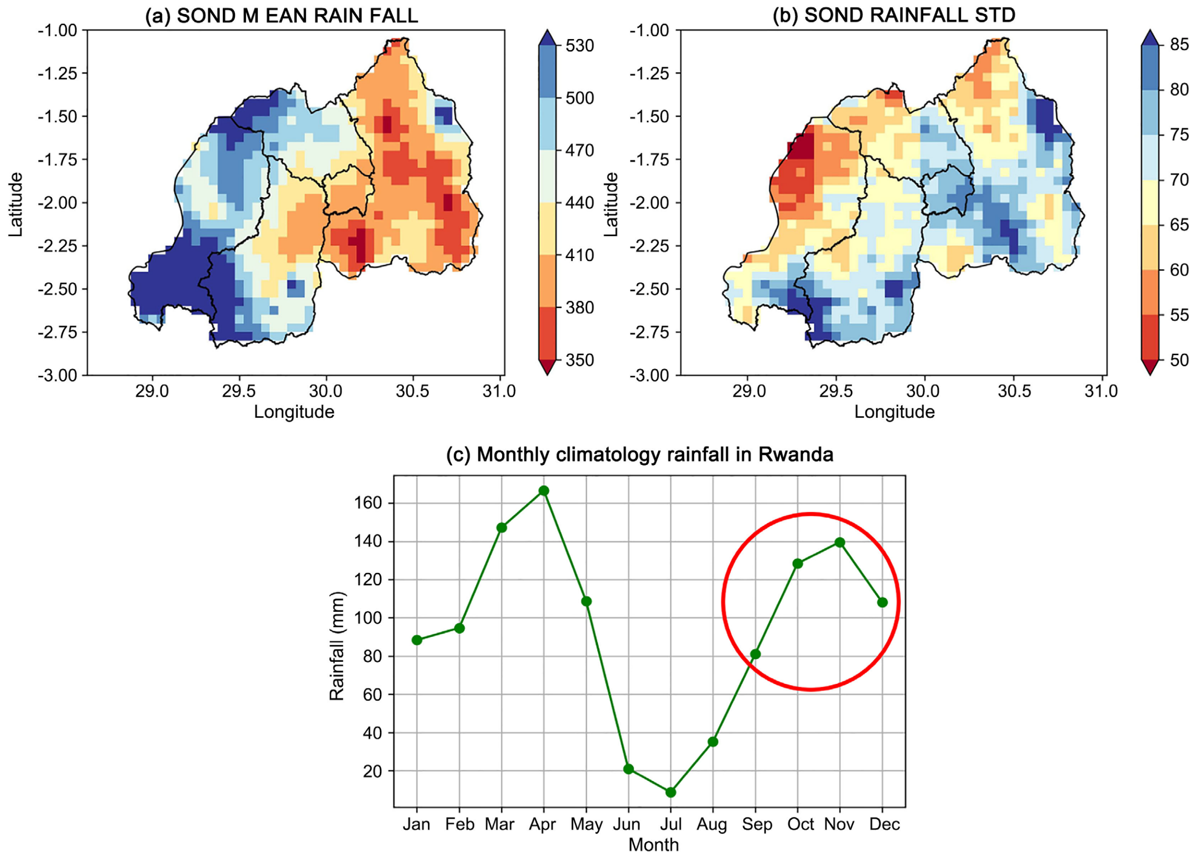

Figure 2. (a) The monthly average rainfall cycle (mm/month), (b) The standard deviation of September to December rainfall in Rwanda (mm/season) and (c) The climatological mean of the September to December rainfall in Rwanda (mm/season).

linked to wet and dry years. Figure 3 below shows the spatial and temporal rainfall anomalies for the first three modes of empirical orthogonal function from deterrent observational data. The results from the analysis brought out 63.6%, 16.5%, and 4.8% of variance in the first, second, and third modes correspondingly. The mode with the highest percentage variance of EOF and its correspondent principal component (first mode of EOF1 and PC1 in (**Figure 3**)) was utilized to select the number of wet and dry years). The area with positive factor loading indicates most variability of rainfall and the area with negative loading represents less variability of rainfall in the country (Martinson, 2018).

3.3. Atmospheric Circulation Anomalies of September to December Rainfall during Abnormal Year

Abnormal Rainfall Years

Figure 4, the standardized principal component (PC1) and standardized rainfall anomalies showed five wet years for a threshold of +1 (1997, 2001, 2011, 2012 and 2020) and five dry years for a threshold of −1 (1993, 1996, 1998, 2007 and 2008). Therefore, the above mentioned wet and dry years were analyzed to capture the rainfall patterns during September to December Abnormal rainfall, Figure 5 shows that during wet years Rwanda experiences abnormal rainfall over most parts of the study area with high significance over eastern, central and south east of the country (doted) while during dry years south western and western highland shows high significance (doted) of receiving less rainfall during September to December season.

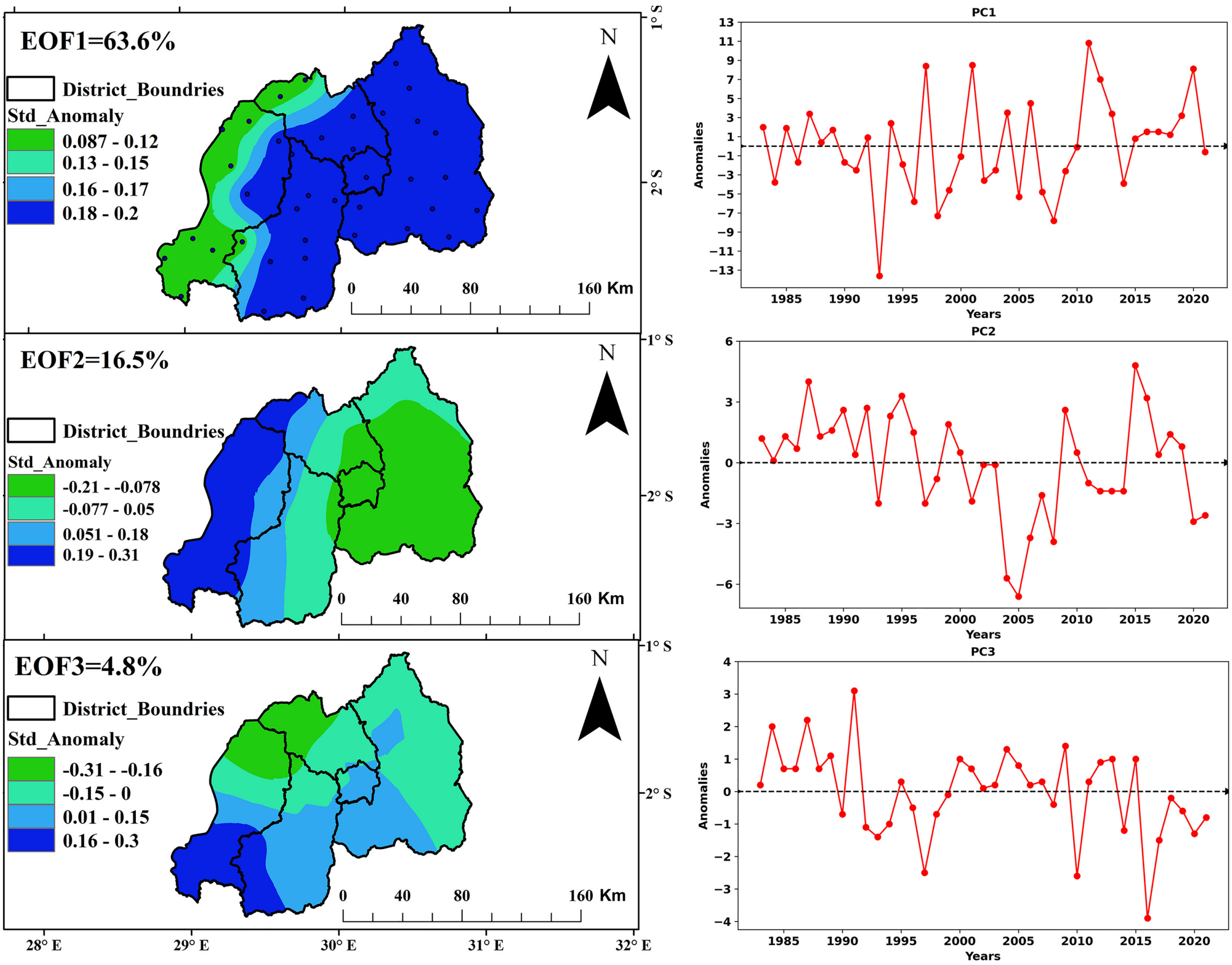

Figure 3. Empirical Orthogonal Function Analysis of rainfall in Rwanda during SOND: EOF patterns (left panel) and their principal components (right panel).

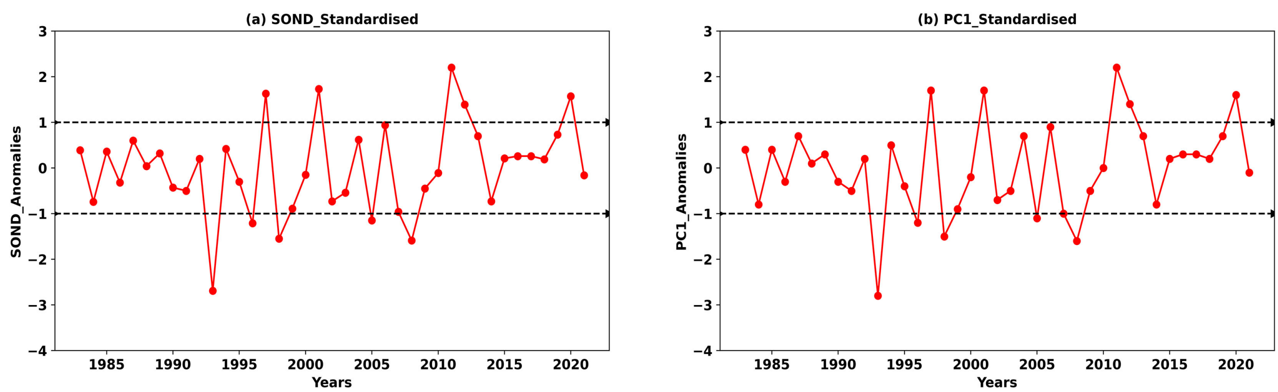

Figure 4. (a) September to December area average rainfall standardized anomaly, (b) The standardized PC1.

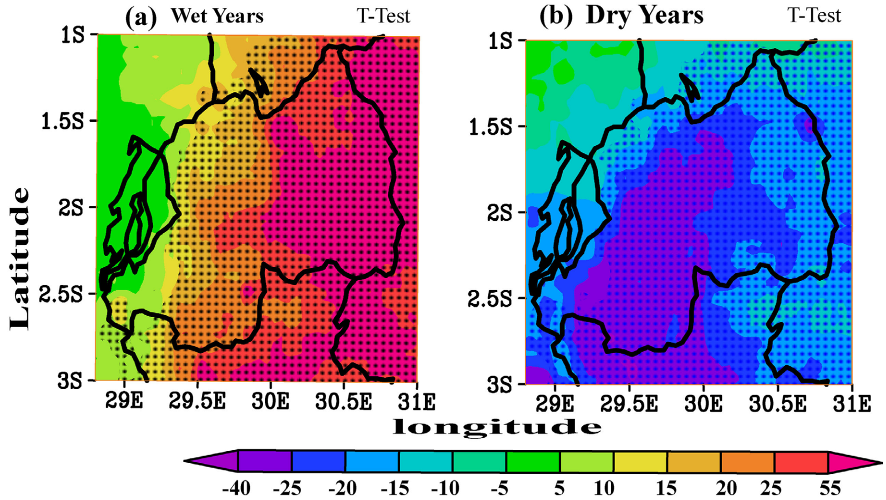

Figure 5. Rainfall (mm/season) anomalies during abnormal (a) wet and (b) dry years, the dotted areas are significant at 95% confidence level.

3.4. Wind Anomaly during Wet and Dry Years

The composite of wind vectors for the wet and dry years at 925 hPa, 850 hPa, 500 hPa and 200 hPa were shown in Figure 6, Figure 7 below where by the shaded areas were significant under statistical test over 95% confidence levels. During the wet years at the low level (925 hPa, 850 hPa) (Figure 6), the easterly winds anomalies were dominated which converge with the south westerly over the study area. These winds originated from Indian Ocean and Congo which normally warm and moist. The remarkable cyclonic circulation of wind anomalies was observed in southern part of the study area which adverting moist wind from the Indian Ocean towards the study area for convection and later favors rainfall also influence the system nearby the coastal area of east Africa. The significant region of 95% confidence level was located within southern, eastern and central of study area.

3.5. The Correlation between the Principal Component (PC1) with Indian Ocean Dipole (IOD) and El-Nino Southern Oscillation (ENSO) Events

Spatial and temporal correlation analysis

The correlation analysis of the precipitation anomaly series with the normalized dipole index (DMI) and the Nino 3.4 index showed that the rainfall in Rwanda from September to December was positively correlated with the Nino 3.4 index (r = 0.15, p value = 0.3, DF = 37), and rainfall was strongly positively correlated with the DMI index (r = 0.43, p value = 0.001, DF = 37). In order to give more insights to the correlation results, the space and time characteristics of PC1 during the various IOD (ENSO) events are presented in this section. Correlation results indicated positive linkages between IOD and seasonal rainfall during the positive Indian Ocean Dipole (PIOD) and Negative Indian Ocean Dipole (NIOD) events over Rwanda (Figure 8).

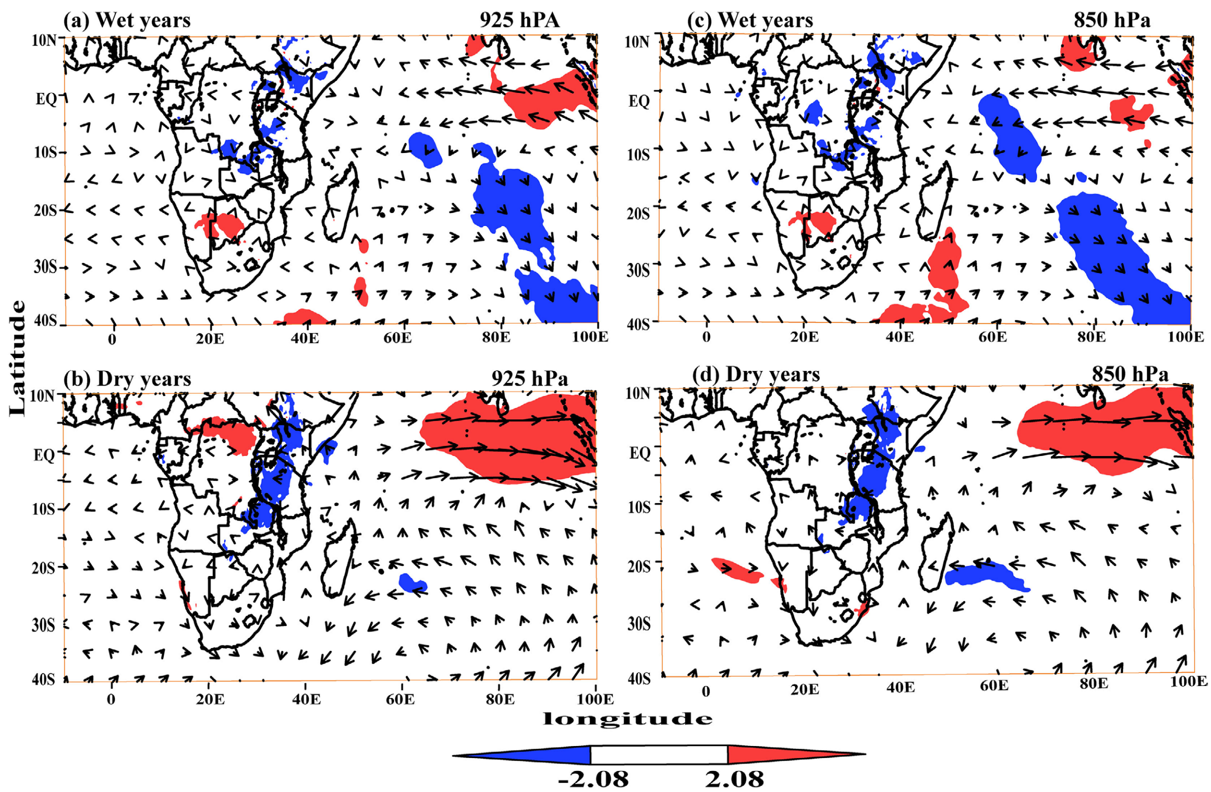

Figure 6. Wind anomalies (m/s) during wet and dry years at 925 hPa and 850 hPa, wind arrows show wind direction while shaded areas show significance at 95% confidence level.

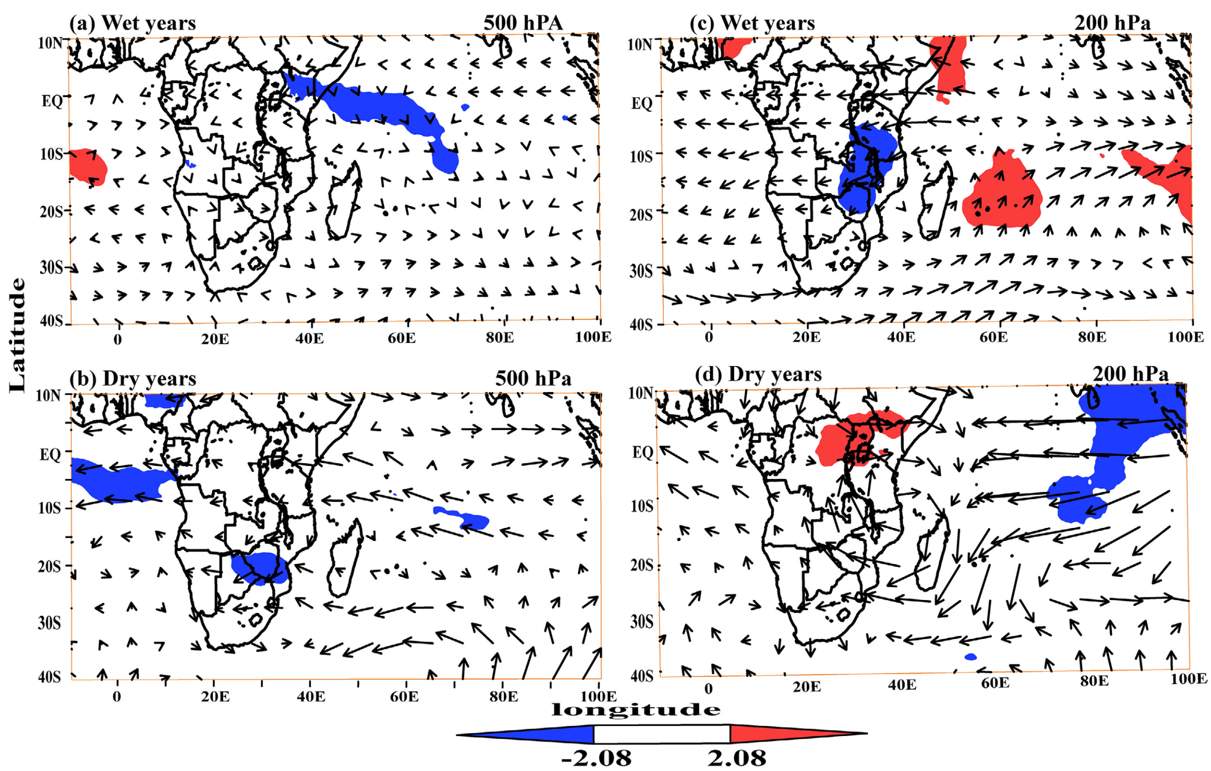

Figure 7. Wind anomalies (m/s) during wet and dry years ((a) & (b)) at 500 hPa and ((c) & (d)) at 200 hPa, wind arrows show wind direction while shaded areas show significance at 95% confidence level.

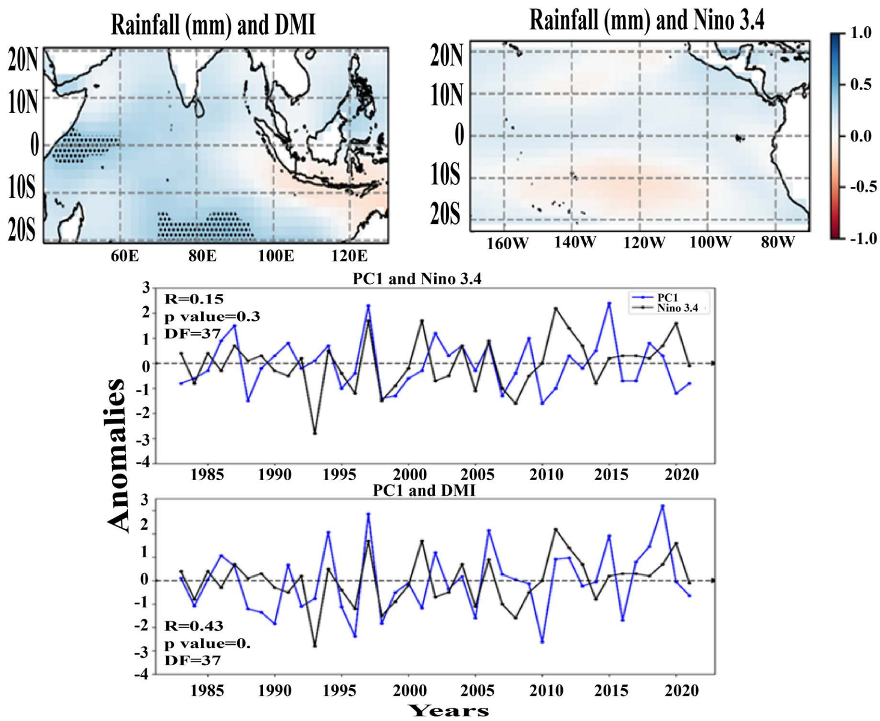

Figure 8. Spatial and temporal correlation analysis between IOD (ENSO) events and PC1, dotted areas are significant at 95% confidence level.

3.6. The Relationship between the Rainfall Anomaly and ENSO/IOD Events

Spatial correlation analysis

Figure 9(a), Figure 9(b) were used to select the El Nino Southern Oscillation (Nino 3.4) and Indian Ocean Dipole (DMI) events from 1983-2021, which were then analyzed through correlation and composite analysis in this study, the spatial correlation coefficient at 95% confidence level was carried out to examine the relationship between September to December rainfall season in Rwanda with September to November Indian Ocean Dipole (IOD) event year and El Nino Southern Oscillation (ENSO) event years. The result therefore shows that, Figure 10(a), there is a strong positive spatial correlation coefficient of precipitation with IOD (DMI) event years and strongly significant at 95% over eastern low land, central plateau and south eastern parts of the country during September to December rain season in Rwanda, the rest of the country exhibits positive correlation coefficient, insignificant. The spatial correlation of the ENSO (Nino 3.4) event years with precipitation in Rwanda Figure 10(b) shows weak positive correlation, insignificant for the September to December rainfall season (1983-2021).

3.7. The Abnormal Circulation Features during Rainfall Abnormal Years

The composite analysis of September to December precipitation anomalies in six kinds of different events are shown in Figure 11. Based on Table 1, single Positive Indian Ocean Dipole (PIOD), Negative Indian Ocean Dipole (NIOD), El

Nino, La Nina, PIOD with El Nino and NIOD with La Nina is plotted. The purpose of the composite is to examine the relationship of Indian Ocean Dipole (IOD) El Nino Southern Oscillation (ENSO) event years and September to December precipitation in Rwanda. The dashed areas Figure 11 are significant at 95% confidence level. The effect of six different events is then easily identified. The rainfall distribution for the IOD (ENSO) events is also shown to easily capture the abnormal rainfall anomaly during September to December rainfall season.

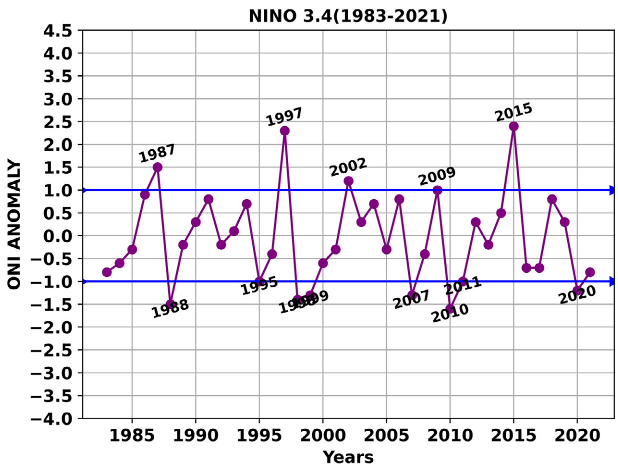

Figure 9. (a) NINO 3.4 and (b) Dipole mode Index (DMI) sea surface anomalies for September to November Months from 1983-2021.

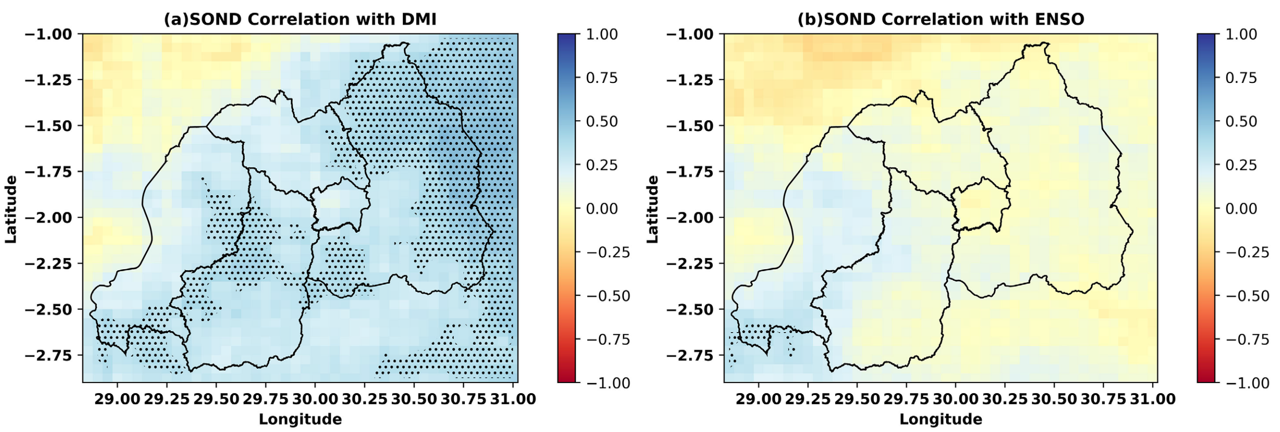

Figure 10. The spatial distribution of correlation coefficient between IOD (ENSO) events and SOND standardized rainfall anomaly in Rwanda, (a) The spatial correlation coefficient of IOD events and precipitation, (b) The spatial correlation coefficient of ENSO events and precipitation, dotted areas are significant at 95% confidence level.

Table 1. IOD (ENSO) event years (1983-2021).

	IOD (ENSO) Event years											
El-Nino	1987 (S)	1997 (PIOD)	2002 (PIOD)	2009 (S)	2015 (PIOD)							
La_Nina	1988 (NIOD)	1995 (NIOD)	1998 (NIOD)	1999 (S)	2007 (S)	2010 (NIOD)	2011 (S)	2020 (S)				
PIOD	1986 (S)	1994 (S)	1997 (E)	2002 (E)	2006 (S)	2015 (E)	2018 (S)	2019 (S)				
NIOD	1984 (S)	1988 (L)	1989 (S)	1990 (S)	1992 (S)	1995 (L)	1996 (S)	1998 (L)	2001 (S)	2005 (S)	2010 (L)	2016 (S)

S = single event; E = El Nino; L = La Nina.

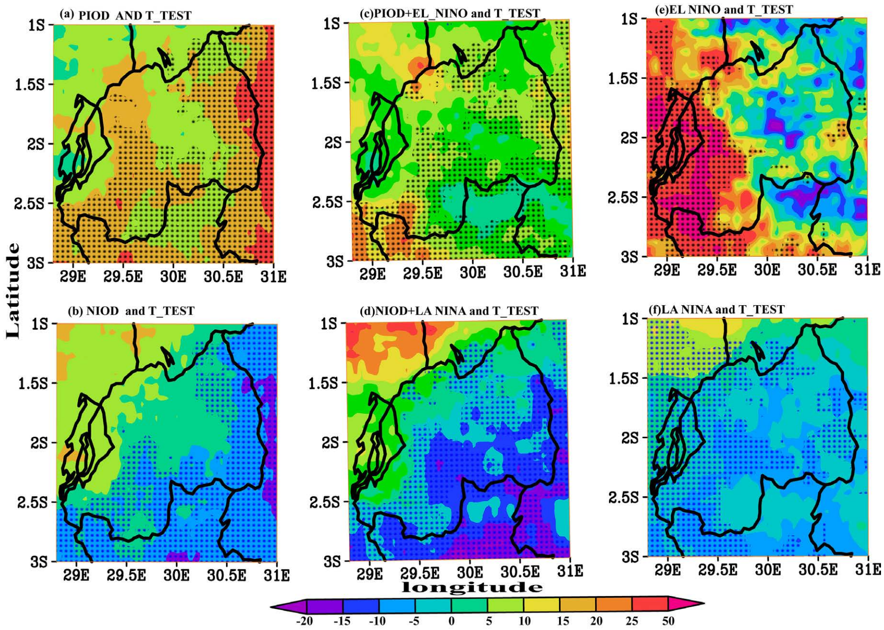

Figure 11. The composite analysis of September to December and spatial precipitation anomaly (mm/season) during IOD (ENSO) years 1983-2021: (a) PIOD, (b) NIOD, (c) PIOD with El Nino concurrent, (d) NIOD with El Nino concurrent (e) El Nino, (f) La Nina. The shaded areas in ((d)-(f)) are statistically significant at 95% confidence level.

3.8. The Mechanisms of the Effect of SSTA Patterns on the Rainfall Anomalies in Rwanda

September to December seasonal rainfall during PIOD, PIOD with El-Nino events Figure 12(a), Figure 12(e) at 850 hPa and Figure 12(c), Figure 12(g) at 200 hPa tropical region is dominated by strong easterlies and southerlies at the surface which allows moisture transport from Indian ocean and westerly wind flow at the upper level, convergence occurs over the study area at the surface. While, during NIOD, NIOD with La-Nina event years Figure 12(b), Figure 12(f) at 850 hPa southerlies area weakened by near equatorial trough which result into the divergence at the surface and convergence Figure 12(d), Figure 12(h) at 200 hPa upper level resulting into downward motion.

3.9. Indian Ocean Walker Circulation during IOD (ENSO) Events

The structure of the vertical velocity (omega) component of the Indian Ocean Walker circulation during IOD (ENSO) events can be seen. The core ascending region over east Africa is strongest during positive Indian Ocean Dipole (PIOD), PIOD with El-Nino events (-0.4 Pa·s^{-1}) and weak during negative Indian Ocean Dipole (NIOD), NIOD with La Nina (0.6 Pa·s^{-1}).

The Indian Ocean Walker Circulation, which is frequently characterized by low-level zonal winds over the equatorial central Indian Ocean, has been connected to East African September to December rains. Similar relationships have been discovered with rainfall-related variables such as lake levels and rainfall. Changes in vertical motion, low-level divergence, and precipitable water volumes over East Africa and the western Indian Ocean accompany an abnormal Walker Circulation, favoring anomalies of the Rwanda September to December (SOND) seasonal rainfall (Zhao & Cook, 2021). **Figure 13(a)** & **Figure 13(c)** show the influence of Indian ocean walker circulation between 20˚E and 60˚E during PIOD (PIOD with El Nino) events there is a persistence of upward motion over western Indian Ocean and east Africa with downward motion over maritime and Austria.

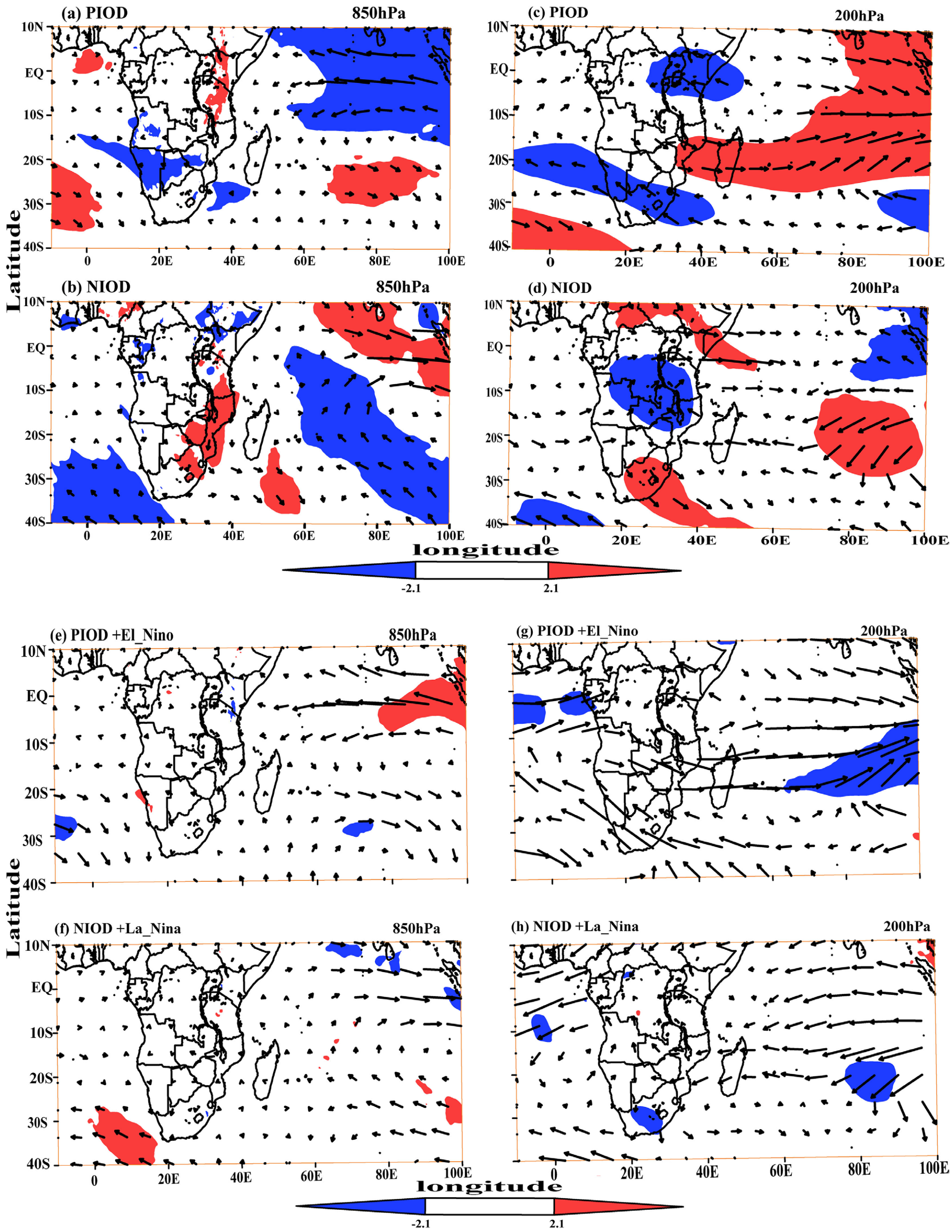

Figure 12. Composites of the wind anomalies (m/s), ((a), (c)) PIOD event years, ((b), (d)) NIOD event years, ((e), (g)) PIOD with El Nino event years, ((f), (h)) NIOD with La Nina event years at 850 hPa and at 200 hPa respectively, shaded areas show significance at 95% confidence level (X and Y axis represent latitude and longitude respectively).

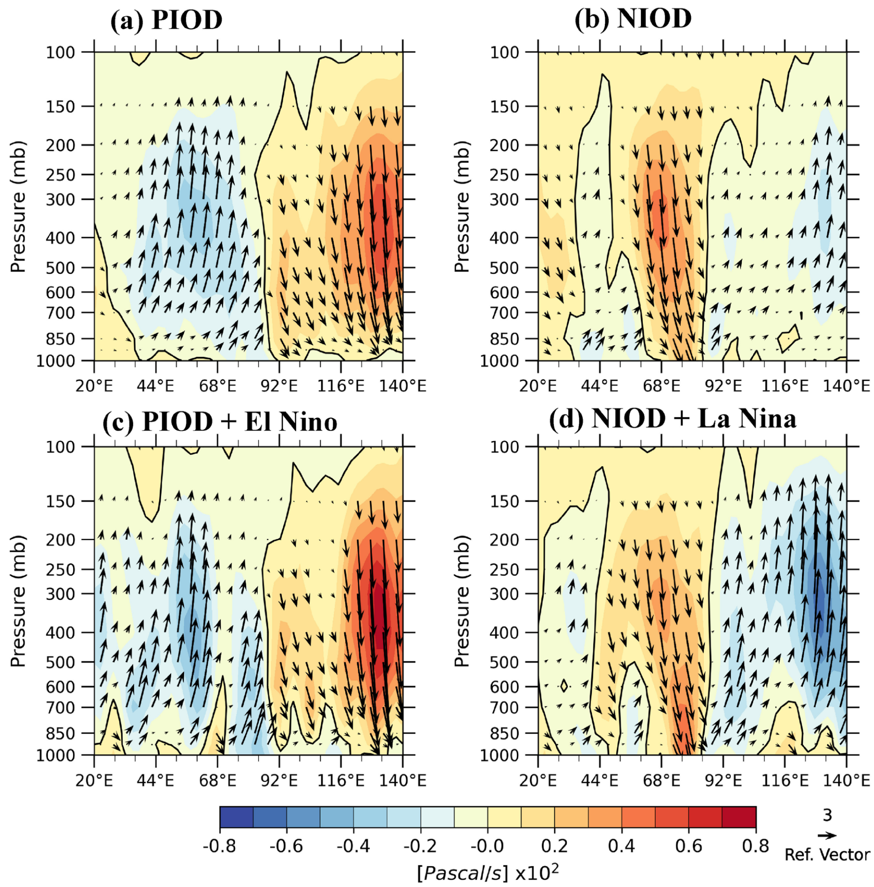

Figure 13. Differences of the Indian walker circulation (vectors) and vertical velocity averaged over 150S (150N), ((a), (c)) PIOD, (PIOD with El Nino) event years, ((b), (d)) NIOD (NIOD with La Nina) event years. The units are (m/s) for zonal wind component and (pa/s) for vertical velocity.

4. Discussion and Conclusion

This study elucidates the intricate relationship between September to December rainfall in Rwanda and the climatic drivers of Indian Ocean Dipole (IOD) and El Niño Southern Oscillation (ENSO) events. Through comprehensive analysis of precipitation data and atmospheric circulation patterns, it is evident that these climate phenomena significantly influence rainfall variability in the Rwanda. The findings highlight the positive correlation between Indian Ocean dipole events and September to December (SOND) seasonal rainfall, as well as the impact of ENSO occurrences, particularly El Niño events, on precipitation patterns. Moreover, the study underscores the importance of considering SSTs and circulation dynamics in forecasting SOND rainfall, with implications for water and agriculture management in Rwanda. By enhancing our understanding of these relationships, this research contributes valuable insights to climate science and informs decision-making processes for mitigating the impacts of climate variability on vulnerable sectors. In addition to elucidating the complex interplay between climatic drivers and SOND rainfall in Rwanda, this study provides critical insights into the implications for future climate projections and adaptation strategies. By highlighting the distinct responses of SOND rainfall to positive and negative phases of Indian Ocean Dipole and El Nino events, the research underscores the need for tailored forecasting models to anticipate potential shifts in precipitation patterns. These findings have profound implications for water resource management, agricultural planning, and disaster preparedness in Rwanda, particularly in light of projected changes in rainfall regimes due to climate change. Furthermore, the study emphasizes the importance of continued monitoring and research efforts to better understand the evolving dynamics of regional climate systems and their impact on socio-economic development. By bridging the gap between scientific knowledge and practical applications, this research serves as a valuable resource for policymakers, stakeholders, and communities striving to build resilience and adapt to a changing climate landscape. Ultimately, the insights gleaned from this study pave the way for informed decision-making and proactive measures to mitigate the adverse effects of climate variability on Rwanda's ecosystems and livelihoods. The study establishes a clear link between September to December (SOND) rainfall in Rwanda and Indian Ocean Dipole (IOD) and El Niño Southern Oscillation (ENSO) events, shedding light on the underlying atmospheric circulation patterns influencing this relationship.

1) Previous research, such as (Akpoti et al., 2016; Asuero et al., 2006; Black, Slingo, & Sperber, 2003), has highlighted the impact of Sea Surface Temperature (SST's) on East Africa Rainfall, reinforcing the significance of considering oceanic conditions in rainfall analysis.

2) Specifically, the findings of this study underscore a strong positive correlation between Indian Ocean dipole events and September to December (SOND) seasonal rainfall in Rwanda, with notable associations with the Nino 3.4 index, indicating El Nino Southern Oscillation (ENSO) influence.

3) Seven out of twenty Indian Ocean dipole events were found to coincide with El Niño Southern Oscillation occurrences, further emphasizing the interconnectedness of these climate phenomena. Significant positive correlations observed between Indian Ocean Dipole and SOND rainfall in various regions of Rwanda at a 95% confidence level affirm the robustness of the relationship.

4) Composite analysis using student T-test demonstrates the substantial impact of Indian Ocean Dipole and El-Nino Southern Oscillation occurrences on SOND rainfall, with PIOD and PIOD with El Nino event year's corresponding to above-normal rainfall and NIOD and NIOD with La Nina event years resulting in below-normal rainfall.

5) Examination of circulation processes during IOD and ENSO events elucidates the atmospheric dynamics driving variations in SOND rainfall, offering valuable insights for forecasting and management strategies in water and agriculture sectors in Rwanda.

The results contribute to the forecasting of the September to December rainfall season in Rwanda in relation to the IOD and ENSO occurrence.

Acknowledgements

The first author is grateful to acknowledge the support from the Chinese Scholarship Council (CSC), the World Meteorological Organization (WMO), Government of Rwanda, Rwanda Defense forces (RDF) and Rwanda Meteorology Agency (Meteo Rwanda) in assisting him in completing his master's degree at Nanjing University of Information Science and Technology. Especially grateful to Professor Ling Zhang for supervising my completion of this paper. The authors thank the prior authors mentioned in the essay for their assistance, as well as the institutions that contributed the rainfall data utilized in the research.

Data Availability Statement

The datasets used on this study are available in the following links:
https://cds.climate.copernicus.eu/cdsapp#!/dataset/reanalysis-era5-single-levels?tab = form;
https://iridl.ldeo.columbia.edu/SOURCES/.UCSB/.CHIRPS/.v2p0/.monthly/.global/index.html?Set-Language = en and
https://psl.noaa.gov/data/gridded/tables/sst.html.

Author Contributions

Frank Rusanganwa is main author of work and Corresponding author; Ling Zhang is Supervisor and coordinate of the work, Jonah Kazora contributed on data and Methodology part, Joseph Ndakize Sebaziga Contributed in research corrections and formatting; Samuel Ekwacu contributed in scripting that used in analysis of this work

Conflicts of Interest

All authors certify that they have no affiliations with or involvement in any organization or entity with any financial interest or non-financial interest in the subject matter or materials discussed in this manuscript.

References

Akpoti, K., Antwi, E., & Kabo-bah, A. (2016). Impacts of Rainfall Variability, Land Use and Land Cover Change on Stream Flow of the Black Volta Basin, West Africa. *Hydrology, 3,* Article No. 26. https://doi.org/10.3390/hydrology3030026

Asuero, A. G., Sayago, A., & González, A. G. (2006). The Correlation Coefficient: An Overview. *Critical Reviews in Analytical Chemistry, 36,* 41-59. https://doi.org/10.1080/10408340500526766

Bayable, G., Amare, G., Alemu, G., & Gashaw, T. (2021). Spatiotemporal Variability and Trends of Rainfall and Its Association with Pacific Ocean Sea Surface Temperature in West Harerge Zone, Eastern Ethiopia. *Environmental Systems Research, 10,* Article No. 7. https://doi.org/10.1186/s40068-020-00216-y

Black, E., Slingo, J., & Sperber, K. R. (2003). An Observational Study of the Relationship between Excessively Strong Short Rains in Coastal East Africa and Indian Ocean SST. *Monthly Weather Review, 131,* 74-94. https://doi.org/10.1175/1520-0493(2003)131<0074:AOSOTR>2.0.CO;2

Blau, M. T., & Ha, K. (2020). The Indian Ocean Dipole and Its Impact on East African Short Rains in Two CMIP5 Historical Scenarios with and without Anthropogenic Influence. *Journal of Geophysical Research: Atmospheres, 125,* e2020JD033121. https://doi.org/10.1029/2020jd033121

Camberlin, P., & Philippon, N. (2002). The East African March-May Rainy Season: Associated Atmospheric Dynamics and Predictability over the 1968-97 Period. *Journal of Climate, 15,* 1002-1019. https://doi.org/10.1175/1520-0442(2002)015<1002:teammr>2.0.co;2

Camberlin, P., Moron, V., Okoola, R., Philippon, N., & Gitau, W. (2009). Components of Rainy Seasons' Variability in Equatorial East Africa: Onset, Cessation, Rainfall Frequency and Intensity. *Theoretical and Applied Climatology, 98,* 237-249. https://doi.org/10.1007/s00704-009-0113-1

Chen, S., Wu, R., & Chen, W. (2018). Modulation of Spring Northern Tropical Atlantic Sea Surface Temperature on the El Niño-Southern Oscillation-East Asian Summer Monsoon Connection. *International Journal of Climatology, 38,* 5020-5029. https://doi.org/10.1002/joc.5710

Clark, C. O., Webster, P. J., & Cole, J. E. (2003). Interdecadal Variability of the Relationship between the Indian Ocean Zonal Mode and East African Coastal Rainfall Anomalies. *Journal of Climate, 16,* 548-554. https://doi.org/10.1175/1520-0442(2003)016<0548:ivotrb>2.0.co;2

Conway, D., Allison, E., Felstead, R., & Goulden, M. (2005). Rainfall Variability in East Africa: Implications for Natural Resources Management and Livelihoods. *Philosophical Transactions of the Royal Society A: Mathematical, Physical and Engineering Sciences, 363,* 49-54. https://doi.org/10.1098/rsta.2004.1475

Fan, L., Liu, Q., Wang, C., & Guo, F. (2017). Indian Ocean Dipole Modes Associated with Different Types of ENSO Development. *Journal of Climate, 30,* 2233-2249. https://doi.org/10.1175/jcli-d-16-0426.1

Gallaudet, T. C., & Simpson, J. J. (1994). An Empirical Orthogonal Function Analysis of Remotely Sensed Sea Surface Temperature Variability and Its Relation to Interior Oceanic Processes off Baja California. *Remote Sensing of Environment, 47,* 375-389. https://doi.org/10.1016/0034-4257(94)90105-8

Gunta, S., Bhat, H. G., & Manjunatha, B. R. (2022). The Response of Geopotential Height Anomalies to El Niño and La Niña Conditions and Their Implications to Seasonal Rainfall Variability over the Horn of Africa. *Atmospheric and Climate Sciences, 12,* 475-492. https://doi.org/10.4236/acs.2022.122028

Jiang, Y., Zhou, L., Roundy, P. E., Hua, W., & Raghavendra, A. (2021). Increasing Influence of Indian Ocean Dipole on Precipitation over Central Equatorial Africa. *Geophysical Research Letters, 48,* e2020GL092370. https://doi.org/10.1029/2020gl092370

Jonah, K., Wen, W., Shahid, S., Ali, M. A., Bilal, M., Habtemicheal, B. A. et al. (2021). Spatiotemporal Variability of Rainfall Trends and Influencing Factors in Rwanda. *Journal of Atmospheric and Solar-Terrestrial Physics, 219,* Article ID: 105631. https://doi.org/10.1016/j.jastp.2021.105631

Li, C., Chai, Y., Yang, L., & Li, H. (2016). Spatio-Temporal Distribution of Flood Disasters and Analysis of Influencing Factors in Africa. *Natural Hazards, 82,* 721-731. https://doi.org/10.1007/s11069-016-2181-8

Liang, X. S. (2014). Unraveling the Cause-Effect Relation between Time Series. *Physical*

Review E, 90, Article ID: 052150. https://doi.org/10.1103/physreve.90.052150

Liu, W., Cook, K. H., & Vizy, E. K. (2020). Influence of Indian Ocean SST Regionality on the East African Short Rains. *Climate Dynamics, 54,* 4991-5011. https://doi.org/10.1007/s00382-020-05265-8

Manatsa, D., Chipindu, B., & Behera, S. K. (2012). Shifts in IOD and Their Impacts on Association with East Africa Rainfall. *Theoretical and Applied Climatology, 110,* 115-128. https://doi.org/10.1007/s00704-012-0610-5

Marchant, R., Mumbi, C., Behera, S., & Yamagata, T. (2007). The Indian Ocean Dipole—The Unsung Driver of Climatic Variability in East Africa. *African Journal of Ecology, 45,* 4-16. https://doi.org/10.1111/j.1365-2028.2006.00707.x

Martinson, D. G. (2018). *Quantitative Methods of Data Analysis for the Physical Sciences and Engineering Empirical Orthogonal Function (EOF) Analysis*.

Mcgregor, G. R. (2018). *El Niño Southern Oscillation (ENSO) and Health: An Overview for Climate and Health Researchers*.

Moihamette, F., Pokam, W. M., Diallo, I., & Washington, R. (2022). Extreme Indian Ocean Dipole and Rainfall Variability over Central Africa. *International Journal of Climatology, 42,* 5255-5272. https://doi.org/10.1002/joc.7531

Ngarukiyimana, J. P., Fu, Y., Yang, Y., Ogwang, B. A., Ongoma, V., & Ntwali, D. (2017). Dominant Atmospheric Circulation Patterns Associated with Abnormal Rainfall Events over Rwanda, East Africa. *International Journal of Climatology, 38,* 187-202. https://doi.org/10.1002/joc.5169

Nicholson, S. E. (2019). A Review of Climate Dynamics and Climate Variability in Eastern Africa. In T. C. Johnson, & E. O. Odada (Eds.), *The Limnology, Climatology and Paleoclimatology of the East African Lakes* (pp. 25-56). Routledge.

Ntirenganya, F. (2016). *Analysis of Rainfall Data from Rwanda Analysis of Rainfall Data from Rwanda*.

Nyenzi, B. S. (1988). *Mechanisms of East African Rainfall Variability*. The Florida State University.

Ogallo, L. J. (1988). Relationships between Seasonal Rainfall in East Africa and the Southern Oscillation. *Journal of Climatology, 8,* 31-43. https://doi.org/10.1002/joc.3370080104

Ongoma, V., Guirong, T., Ogwang, B., & Ngarukiyimana, J. (2015). Diagnosis of Seasonal Rainfall Variability over East Africa: A Case Study of 2010-2011 Drought over Kenya. *Pakistan Journal of Meteorology, 11,* 13-21.

Piao, J., Chen, W., Chen, S., Gong, H., Chen, X., & Liu, B. (2020). The Intensified Impact of El Niño on Late-Summer Precipitation over East Asia since the Early 1990s. *Climate Dynamics, 54,* 4793-4809. https://doi.org/10.1007/s00382-020-05254-x

Saji, N. H., Goswami, B. N., Vinayachandran, P. N., & Yamagata, T. (1999). A Dipole Mode in the Tropical Indian Ocean. *Nature, 401,* 360-363. https://doi.org/10.1038/43854

Shi, W., & Wang, M. (2021). A Biological Indian Ocean Dipole Event in 2019. *Scientific Reports, 11,* Article No. 2452. https://doi.org/10.1038/s41598-021-81410-5

Stern, R. D., & Cooper, P. J. M. (2011). Assessing Climate Risk and Climate Change Using Rainfall Data—A Case Study from Zambia. *Experimental Agriculture, 47,* 241-266. https://doi.org/10.1017/s0014479711000081

Uwimbabazi, J., Jing, Y., Iyakaremye, V., Ullah, I., & Ayugi, B. (2022). Observed Changes in Meteorological Drought Events during 1981-2020 over Rwanda, East Africa. *Sustainability, 14,* Article No. 1519. https://doi.org/10.3390/su14031519

Wainwright, C. M., Finney, D. L., Kilavi, M., Black, E., & Marsham, J. H. (2020). Extreme Rainfall in East Africa, October 2019-January 2020 and Context under Future Climate Change. *Weather, 76,* 26-31. https://doi.org/10.1002/wea.3824

Webster, P. J., Moore, A. M., Loschnigg, J. P., & Leben, R. R. (1999). Coupled Ocean-Atmosphere Dynamics in the Indian Ocean during 1997-98. *Nature, 401,* 356-360. https://doi.org/10.1038/43848

Yang, S., Li, Z., Yu, J., Hu, X., Dong, W., & He, S. (2018). El Niño-Southern Oscillation and Its Impact in the Changing Climate. *National Science Review, 5,* 840-857. https://doi.org/10.1093/nsr/nwy046

Zhang, L., Shi, R., Fraedrich, K., & Zhu, X. (2022). Enhanced Joint Effects of ENSO and IOD on Southeast China Winter Precipitation after 1980s. *Climate Dynamics, 58,* 277-292. https://doi.org/10.1007/s00382-021-05907-5

Zhao, S., & Cook, K. H. (2021). Influence of Walker Circulations on East African Rainfall. *Climate Dynamics, 56,* 2127-2147. https://doi.org/10.1007/s00382-020-05579-7